ORGANOMETALLICS

Article

pubs.acs.org/Organometallics

Donor–Acceptor Properties of Bidentate Phosphines. DFT Study of Nickel Carbonyls and Molecular Dihydrogen Complexes

Charity Flener Lovitt,[†] Gernot Frenking,*[,‡] and Gregory S. Girolami*[,†]

[†]School of Chemical Sciences, University of Illinois at Urbana–Champaign, 600 South Mathews Avenue, Urbana, Illinois 61801, United States

[‡]Fachbereich Chemie, Philipps-Universität Marburg, Hans Meerwein-Strasse, D-35043 Marburg, Germany

Supporting Information

ABSTRACT: Density functional theory (DFT) is used to investigate the geometries and metal–ligand bonding in nickel complexes of bidentate phosphines, $NiX_2(R_2P(CH_2)_nPR_2)$, where X = H, CO, n = 1–3, and R = H, Me, CF_3, Et, i-Pr, t-Bu, Ph, OMe, F. The net donor–acceptor properties of the phosphine ligands can be deduced from the computed frequency of the symmetric CO stretch of the $Ni(CO)_2(R_2P(CH_2)_nPR_2)$ carbonyl complexes. This frequency (in cm^{-1}) can be estimated from the empirical expression $\nu(CO) = 1988 + \sum\chi_B - 4n$, where the sum is over the four substituents on the bidentate phosphine, χ_B is a substituent-dependent parameter, and n is the number of carbon atoms in the backbone ($1 \le n \le 3$). The deduced values of χ_B (in units of cm^{-1})—t-Bu (0.0), i-Pr (0.8), Et (3.0), Me (4.0), Ph (4.3), H (6.3), OMe (10.8), CF_3 (17.8), and F (18.3)—are generally similar to Tolman's electronic parameter χ derived from nickel complexes of unidentate phosphines. For the $NiH_2(R_2P(CH_2)_nPR_2)$ hydride complexes, the global minimum is a nonclassical dihydrogen structure, irrespective of the nature of the phosphine. For bidentate phosphines that are strongly donating, a classical *cis*-dihydride structure lies higher in energy (in some cases, by only 0.4 kcal mol^{-1} above the global minimum). For phosphines that are less electron donating, the dihydride structure is no longer a local minimum but instead is an inflection point on the potential energy surface. Atoms in molecules (AIM) and natural bond order (NBO) analyses confirm that the nickel–dihydrogen interaction involves a three-center–two-electron bond. The Kohn–Sham molecular orbital diagram and energy decomposition analysis of these complexes show that metal to H_2 π back-donation is the dominant orbital component for phosphines with electron-donating substituents, whereas H_2 to metal σ donation is dominant for phosphines with electron-withdrawing substituents. The EDA results clearly indicate that long H–H distances are seen when the metal to H_2 π back-donation dominates over H_2 to M σ donation.

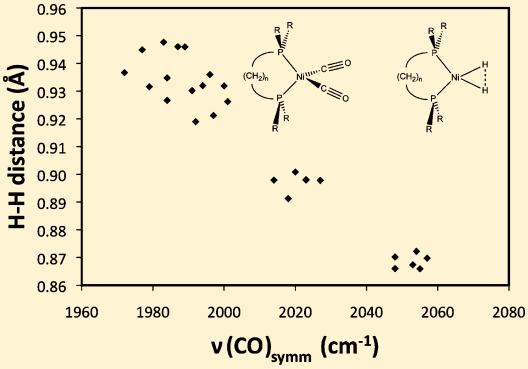

1. INTRODUCTION

Bidentate phosphines are immensely important auxiliary ligands for transition metals. Their usefulness stems in part from their ability to create a relatively rigid steric environment that can impose specific constraints on the relative positions (e.g., cis vs trans) as well as the conformations of other ligands that bind to the metal center. In addition, the electron-donating properties of the bidentate phosphine can alter the electron richness of the metal center, which in turn affects the binding and reactivity of the other ligands. These factors can greatly enhance the regiospecificity, stereospecificity, and rate of reactions catalyzed by transition metals. A detailed understanding of the influence of bidentate phosphines on the steric and electronic properties of their metal complexes is therefore of great importance.

There have been many experimental[1] and theoretical[2−4] studies of the bonding of unidentate phosphines to transition metals, but there are very few such studies of bidentate phosphines. The effect of the phosphorus-bound substituents on the steric and electronic properties of bidentate phosphines has generally been assumed to be identical with the effect of the same substituents in unidentate phosphines, but there is some evidence that this assumption is not true. For example, metal–substrate bond dissociation energies are slightly different for metal complexes of bidentate phosphines relative to those of their unidentate phosphine counterparts.[5] A few studies have compared metal–ligand bonding in a small number of bidentate phosphines,[5,6] but no rigorous studies have been undertaken for a wide range of bidentate complexes. In addition, it is well appreciated that the P–M–P angles in complexes of bidentate phosphines are often quite different from those seen for complexes of unidentate phosphines, and this geometric difference may also have electronic consequences.

The most widely employed experimental measure of the donor–acceptor properties of a unidentate phosphine (and many other kinds of ligands) is the Tolman electronic parameter, which is equal to the CO stretching frequency of

Received: May 27, 2011
Published: May 30, 2012

   dx.doi.org/10.1021/om200456j | *Organometallics* 2012, 31, 4122–4132

A_1 symmetry in the corresponding $Ni(CO)_3L$ complex.[1] The CO stretching frequency correlates well with the net donor ability of the ligand L to a metal center in other systems.[7] Tolman showed that the electronic parameter ν of a phosphine $PX_1X_2X_3$ could be predicted reasonably accurately from the identities of the three substituents via the equation

$$\nu = 2056.1 + \sum_{i=1}^{3} \chi_i \quad (1)$$

where χ_i is an empirically derived number characteristic of the substituent X_i. Crabtree and co-workers determined that ligand electron parameters of $Ni(CO)_3L$ complexes computed by DFT methods correlate well not only with the Tolman parameters but also with other experimental gauges of electron donor−acceptor properties such as Lever parameters derived from redox potentials and Hammett constants derived from NMR chemical shifts.[4] Computed electronic parameters have been used in the past to augment experimental Tolman parameters.[2,8]

The Tolman electronic parameters provide information about the net donor ability of the ancillary ligands; i.e., they take into account both σ and π metal−ligand bonding. One method to disentangle the σ and π components of the metal−ligand bonding is to analyze the results of DFT calculations with techniques such as natural bond orbital analysis (NBO), Bader's atoms in molecule (AIM) approach, and energy decomposition analysis (EDA). NBO converts the molecular wave functions generated by Hartree−Fock and Kohn−Sham methods into core orbitals, bonding orbitals, and lone electron pairs localized on the molecular structure.[9,10] This type of analysis has been applied to describing the bonding in transition-metal complexes.[11] Bader's AIM method, which uses the Laplacian of the electron density to identify regions of enhanced or depleted electron density,[12] has proven useful in analyzing the bonding in weakly interacting systems.[13] The AIM approach defines "bond critical points" to be saddle points in the electron density located between nuclei and "bond paths" to be lines of steepest descent in $\rho(\vec{r})$ that connect nuclei with the bond critical points.[12]

EDA, which describes bond formation in terms of a collection of interacting fragments, has also been regularly applied to donor−acceptor complexes of transition metals and main-group elements.[5,14,15] Mathematically[16−22] the bond energy (dissociation energy) of a molecule is assumed to be equal to the sum of two terms, a preparation energy and an interaction energy:

$$D_e = \Delta E_{prep} + \Delta E_{int} \quad (2)$$

The preparation energy is the energy required to promote the relaxed fragments into the geometry and spin state necessary for forming the bond with no further change in geometry. The interaction energy is divided into three parts — the electrostatic term, the Pauli term, and the orbital term—as follows:

$$\Delta E_{int} = \Delta E_{elstat} + \Delta E_{Pauli} + \Delta E_{orb} \quad (3)$$

The electrostatic term is the calculated electrostatic interaction energy between the frozen fragments of the molecule, which is in most cases strongly attractive even for nonpolar molecules. The Pauli term, which gauges the repulsive four-electron interactions between occupied orbitals, arises from the antisymmetry required in the wave function. The orbital interaction term can be regarded as an estimate of the attractive interactions that arise from covalent mixing between the occupied and unoccupied orbitals of the fragments. The key benefit of EDA is that the orbital interaction term can differentiate between σ and π interactions, provided that the molecule processes sufficient molecular symmetry. Because the interaction and orbital terms can be decomposed into physically meaningful components, EDA allows the bonding to be evaluated comprehensively.[7,15,23]

Here, we carry out DFT calculations on bidentate phosphine complexes of stoichiometry $Ni(CO)_2(R_2P(CH_2)_nPR_2)$, where n = 1−3 and R = H, Me, CF_3, Et, i-Pr, t-Bu, Ph, OMe, F, as shown in Scheme 1.

Scheme 1

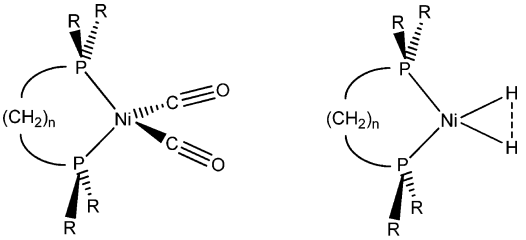

We gauge the donor ability of the bidentate phosphine from the computed CO stretching frequencies in the carbonyl complexes and compare our results with available experimental data and with the properties of unidentate phosphine ligands bearing the same terminal substituents on phosphorus.

In order to exploit these results, we examine how the donor−acceptor properties of the bidentate phosphine ligand affect the structures and dynamics of nickel hydride complexes of stoichiometry $NiH_2(R_2P(CH_2)_nPR_2)$. As we will show, our calculations reveal that these compounds exist as nonclassical dihydrogen complexes (H−H distance <1.0 Å). Depending on the phosphine, in some cases there is a higher energy classical dihydride structure (H−H distance >1.5 Å). We also investigate hydrogen exchange mechanisms in this system and show them to be very sensitive to steric and electronic effects.

2. COMPUTATIONAL METHODS

The structures of all phosphine complexes were optimized without symmetry constraints in Turbomole 6.0[24] using gradient-corrected density functional theory (DFT) at the BP86[25,26] level in conjunction with the "resolution of identity" approximation[27] (RI-BP86) and the def2-TZVP basis set[28] on all atoms using tight convergence criteria ($SCFConv = 8). BP86 was chosen after we carried out scans of one molecule, $NiH_2(H_2PCH_2PCH_2)$, using several functionals (BP86, B3LYP, M05-2X, and PBE0; see the Supporting Information). The results of these scans are similar, with the exception of M05-2X, which gives energies slightly different from those of the other functionals; otherwise, the results from BP86 are representative. This finding is consistent with other theoretical studies[29] of transition-metal compounds, which show that BP86 generally gives accurate results.[30,31] Except when noted, all structures are local minima on the potential energy surface, as confirmed by analytic frequency calculations. Nickel complexes bearing bidentate phosphines with one or three CH_2 groups in the backbone generally optimize to a structure that possesses near-ideal mirror symmetry, in which the mirror plane passes through the Ni atom and the central CH_2 group of the phosphine backbone. Nickel complexes with two CH_2 groups in the backbone generally optimize to a structure with near-ideal C_2 symmetry, in which the C_2 axis passes through the Ni atom and between the two CH_2 groups on the phosphine backbone. Some small

dx.doi.org/10.1021/om200456j | Organometallics 2012, 31, 4122−4132

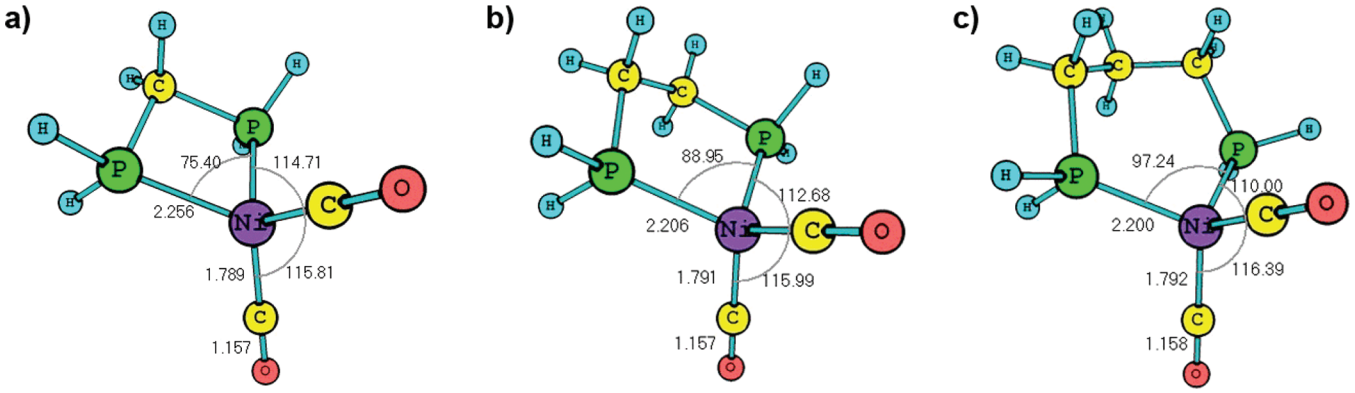

Figure 1. Structures of (a) $Ni(CO)_2(H_2PCH_2PH_2)$ (dhpmCO). (b) $Ni(CO)_2(H_2PCH_2CH_2PH_2)$ (dhpeCO), and (c) $Ni(CO)_2(H_2PCH_2CH_2CH_2PH_2)$ (dhppCO).

Table 1. Geometric and Vibrational Data for $Ni(CO)_2(PR_3)_2$ and $Ni(CO)_2(R_2P(CH_2)_nPR_2)$ Complexes Optimized with RI-BP86/def2-TZVP

label	n	R	C–O_{av} (Å)	Ni–C_{av} (Å)	Ni–P_{av} (Å)	P–Ni–P (deg)	C–Ni–C (deg)	$\nu(CO)_{sym}$ (cm^{-1})	$\nu(CO)_{asym}$ (cm^{-1})
PH_3CO		H	1.157	1.792	2.212	106.0	116.0	2022	1985
PMe_3CO		Me	1.162	1.782	2.222	110.7	116.7	1988	1951
PPh_3CO		Ph	1.160	1.783	2.255	104.5	114.9	1992	1958
$PtBu_3CO$		t-Bu	1.166	1.778	2.436	133.6	115.1	1961	1921
dtbupmCO	1	t-Bu	1.163	1.778	2.295	78.0	111.2	1984	1946
dtbupeCO	2	t-Bu	1.163	1.780	2.266	92.0	107.1	1977	1940
dtbuppCO	3	t-Bu	1.164	1.780	2.279	103.5	107.8	1972	1934
diprpmCO	1	i-Pr	1.162	1.779	2.260	76.3	115.3	1987	1951
diprpeCO	2	i-Pr	1.163	1.780	2.240	90.8	112.9	1983	1946
diprppCO	3	i-Pr	1.163	1.781	2.235	98.0	110.6	1979	1943
depmCO	1	Et	1.161	1.780	2.255	76.1	114.8	1994	1956
depeCO	2	Et	1.162	1.780	2.218	90.3	116.2	1989	1952
deppCO	3	Et	1.162	1.782	2.219	99.1	113.9	1984	1948
dmpmCO	1	Me	1.161	1.782	2.253	76.1	116.0	2000	1962
dmpeCO	2	Me	1.161	1.783	2.213	90.1	116.2	1996	1959
dmppCO	3	Me	1.162	1.782	2.209	99.2	115.9	1991	1954
dppmCO	1	Ph	1.160	1.783	2.259	75.6	113.8	2001	1960
dppeCO	2	Ph	1.160	1.785	2.228	89.9	112.2	1997	1963
dpppCO	3	Ph	1.162	1.783	2.222	98.8	111.1	1992	1958
dhpmCO	1	H	1.157	1.788	2.256	75.4	115.8	2023	1985
dhpeCO	2	H	1.157	1.791	2.206	89.0	116.0	2020	1983
dhppCO	3	H	1.158	1.790	2.200	97.2	116.4	2014	1977
domepmCO	1	OMe	1.156	1.790	2.200	75.4	114.5	2027	1990
domepeCO[a]	2	OMe	1.157	1.792	2.169	89.5	114.7	2023	1987
domeppCO	3	OMe	1.158	1.790	2.166	98.4	115.1	2018	1980
dcf3pmCO	1	CF_3	1.151	1.802	2.221	76.1	113.0	2055	2022
dcf3peCO	2	CF_3	1.151	1.804	2.175	88.9	112.0	2053	2021
dcf3ppCO	3	CF_3	1.152	1.804	2.172	98.4	110.8	2048	2016
dfpmCO	1	F	1.151	1.802	2.179	75.1	111.3	2057	2022
dfpeCO	2	F	1.152	1.803	2.143	88.5	112.1	2054	2020
dfppCO	3	F	1.152	1.808	2.172	96.9	113.2	2048	2013

[a]The optimized complex exhibits one imaginary frequency at −32 cm^{-1}.

deviations from these symmetries are seen when the phosphine ligand bears very large substituents such as t-Bu, but otherwise the nickel complexes can be optimized by constraining the symmetry to be either C_s or C_2 to give structures and energies that are essentially identical with those obtained in the absence of constraints. Vibrational frequencies reported for the complexes are unscaled.

The energy of the relaxed $NiH_2(H_2PCH_2PCH_2)$ complex as a function of the H–H distance (referred to as the relaxed H–H scan) was performed in Gaussian03 Rev. E.01 at the BP86/def2-TZVP[28] level. Natural bond orbitals were obtained using NBO 3.1[9] as implemented in Gaussians03 Rev. E.01.[32] NBO electron densities were generated from single-point calculations of the molecules with BP86/def2-TZVP basis sets in Gaussian03 from Turbomole 6.0 optimized geometries.

Density plots for Bader analysis were generated using the tm2 molden and molden2wfn utilities; the wave function files for the plots were generated from the Turbomole structures and were optimized without symmetry constraints. Contour plots were created using AIMPAC.[12] The energy decomposition analysis was performed using the Amsterdam Density Functional[33] program ADF 2006.01b; the

dx.doi.org/10.1021/om200456j | *Organometallics* 2012, 31, 4122–4132

Turbomole structures were reoptimized with the symmetry constrained to C_2 (n = 2) or C_s (n = 1 or 3), and BP86 and Slater type orbitals were used with the zeroth-order regular approximation (ZORA) for estimating relativistic effects.[34−37] These structures, which were only slightly higher in energy (<0.005 kcal mol^{-1}) than the nonsymmetrized structures, agree well with Turbomole geometries, except that the H−H distance within the dihydride tautomers varies somewhat because the potential energy surface is unusually flat along this structural coordinate.

3. Ni(CO)$_2$(R$_2$P(CH$_2$)$_N$PR$_2$) COMPLEXES

Geometries. DFT calculations using the basis sets and functionals described in Computational Methods were employed to optimize the structures of the following nickel carbonyl complexes bearing bidentate phosphines: Ni(CO)$_2$(R$_2$P(CH$_2$)$_n$PR$_2$), where n = 1−3 and R = H, Me, CF$_3$, Et, i-Pr, t-Bu, Ph, OMe, F. For comparison, we also determined optimized structures for two nickel carbonyl complexes of unidentate phosphines, Ni(CO)$_2$(PMe$_3$)$_2$ and Ni(CO)$_2$(PPh$_3$)$_2$. All of these compounds adopt the distorted-tetrahedral geometries expected for four-coordinate complexes of Ni^0 (Figure 1).[38,39] Data for all structures can be found in Table 1. The calculated C−O bond distances are slightly longer than those determined crystallographically. For example, the calculated CO bond distance of Ni(CO)$_2$[(t-Bu)$_2$PCH$_2$P(t-Bu)$_2$] is 1.163 Å, which is 0.02 Å longer than the experimental bond distance of 1.143 Å;[40,41] the latter may be affected by librational effects.

The calculated P−Ni−P angles increase by ∼12° for each CH$_2$ group added to the phosphine backbone and are 75−78, 88−91, and 98−103° for n = 1−3, respectively. For molecules with identical phosphine substituents R, the Ni−P distance is 0.03 Å longer when the backbone has one CH$_2$ group vs when there are two or three groups (which have essentially identical Ni−P bond lengths). Evidently, the small P−Ni−P angle for the R$_2$P−CH$_2$−PR$_2$ phosphines leads to poorer overlap between nickel and phosphorus. For a given backbone length, the P−Ni−P angle is affected by steric effects: it is slightly larger if the terminal substituents R are larger. Thus, of the complexes we studied, the smallest P−Ni−P angle is seen for the complexes with R = F and the largest for complexes with R = t-Bu. As expected, the calculated P−Ni−P angle of 110° in Ni(CO)$_2$(PMe$_3$)$_2$ is larger than in any of the bidentate phosphine complexes studied. The P−Ni−C and C−Ni−C angles in all of these molecules lie close to the ideal tetrahedral value of 109.5°.

For each optimized structure, symmetric and asymmetric CO stretching frequencies were calculated and compared with those determined experimentally[38,42,43] and theoretically.[5] The symmetric carbonyl stretching frequencies are strongly correlated in the expected way with the C−O and Ni−C bond lengths: higher frequencies correspond to shorter C−O bonds and longer Ni−C bonds. Our calculated values generally match the experimental trends seen in these complexes, with a correlation coefficient of 0.942 (Figure 2). We are doubtful that the less than perfect matching of calculated and experimental IR stretching frequencies in Figure 2 reflects the inability of the calculations to make accurate predictions, though we cannot rule this possibility out. Alternatively, the discrepancies could reflect variations in the experimental conditions, because the data were obtained from samples in different solvents and mulling agents.

Substituent Effects in Bidentate Phosphines. In a fashion similar to Tolman's approach for unidentate phosphines, it is possible to devise an empirical equation to predict the symmetric CO stretching frequencies for Ni(CO)$_2$(R$_2$P(CH$_2$)$_n$PR$_2$) complexes, given the identities of the phosphorus-bound substituents and the length of the backbone. This equation is $\nu(CO) = 1982 + \sum\chi_B - 4n$, where χ_B is substituent dependent and n is the number of carbon atoms in the phosphine backbone ($1 \le n \le 3$). Here, the frequencies are in wavenumbers and the subscript B in χ_B denotes that the substituent parameters are for bidentate phosphines.

The deduced values of χ_B (in units of cm^{-1}) for different substituents are given in Table 2. The χ_B values for the various substituents follow the same trends as do Tolman's χ values for the same substituents in unidentate phosphines, but there are some small differences. For example, almost all the χ_B values are larger than the corresponding Tolman parameter χ for the same substituent. This trend may be a consequence of our deducing the χ_B values from nickel dicarbonyl complexes, whereas the Tolman χ values are deduced from nickel tricarbonyl complexes. In other words, the electronic effects of the phosphine substituents are distributed over two carbonyl groups for χ_B but over three for χ. We should expect the substituents to exert a larger effect on the carbonyl frequencies in the former case than in the latter. To test this idea, we carried out calculations on a few Ni(CO)$_2$(PR$_3$)$_2$ complexes of unidentate phosphines. From the calculated frequencies in

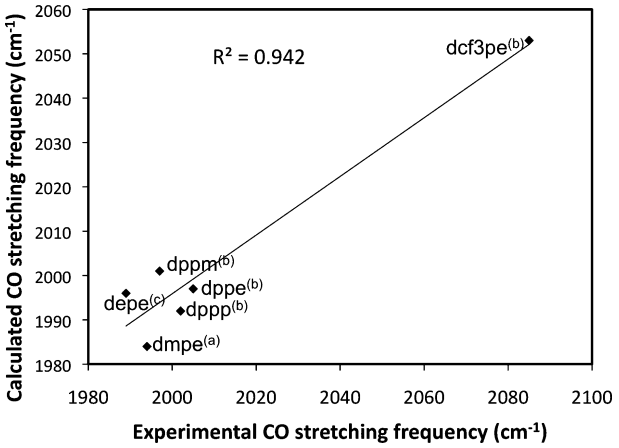

Figure 2. Comparison between experimental and calculated symmetric ν(CO) stretching frequencies of Ni(CO)$_2$(R$_2$P(CH$_2$)$_n$PR$_2$) complexes: (a) ref 42; (b) ref 43; (c) ref 44.

Table 2. Comparison of Tolman's Electronic Substituent Parameters χ for Unidentate Phosphines and the Corresponding Substituent Parameters χ_B for Bidentate Phosphines

substituent	χ,[a] cm^{-1}	χ_B,[b] cm^{-1}
tBu	0.0	0.0
iPr	1.0	1.3
Et	1.8	2.8
Me	2.6	4.5
Ph	4.3	4.8
H	8.3	10.3
OMe	7.7	11.3
CF$_3$	19.6	18.6
F	18.2	18.8

[a]From Tolman.[1] [b]From the current work.

dx.doi.org/10.1021/om200456j | Organometallics 2012, 31, 4122−4132

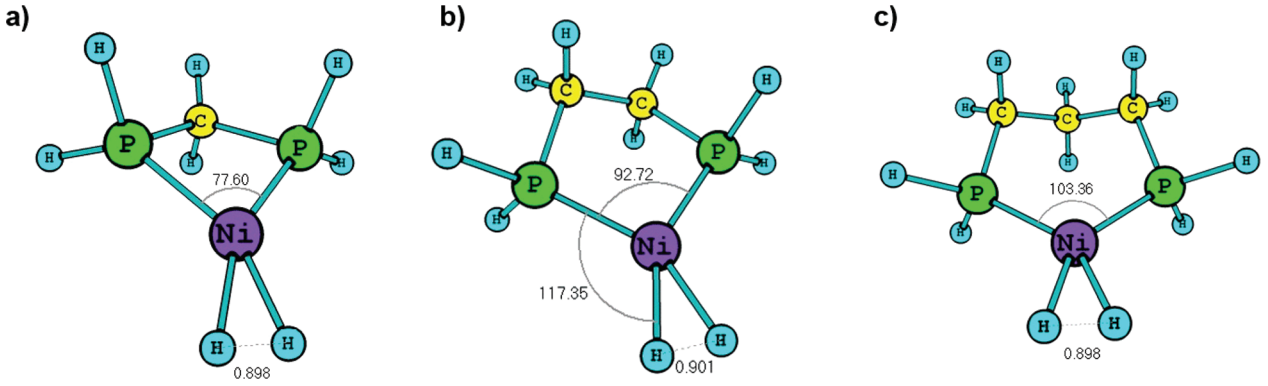

Figure 3. Structures of (a) $Ni(H_2)(H_2PCH_2PH_2)$ (dhpmH2), (b) $Ni(H_2)(H_2PCH_2CH_2PH_2)$ (dhpeH2), and (c) $Ni(H_2)(H_2PCH_2CH_2CH_2PH_2)$ (dhppH2).

Table 1 for these unidentate phosphine complexes, we can deduce the following substituent parameters (in units of cm^{-1}): t-Bu (0.0), Me (4.5), Ph (5.2), and H (10.2). These values are essentially identical with those deduced from the calculated CO stretching frequencies of the $Ni(CO)_2(R_2P(CH_2)_nPR_2)$ complexes. Thus, we conclude that substituents have the same relative effect on the donor–acceptor properties of unidentate phosphines as they do on bidentate phosphines. The data also suggest that the small differences between Tolman's χ parameters and the χ_B values derived here are due in part to the fact that the former are derived from $Ni(CO)_3(PR_3)$ complexes, whereas the latter are derived from $Ni(CO)_2(PR_3)_2$ complexes.

Interestingly, there are some differences between χ_B (obtained from the calculated stretching frequency of a $Ni(CO)_2(R_2P(CH_2)_nPR_2)$ complex) and χ (obtained from the experimental stretching frequency of a $Ni(CO)_3(PR_3)$ complex) that cannot be explained in terms of the different number of carbonyl groups on nickel. One difference is that the χ_B value of methyl and phenyl differ by only 0.3 cm^{-1}, whereas the χ (Tolman) values of these two groups differ by 1.7 cm^{-1} (recall that these values are per R substituent, so that the symmetric CO stretching frequencies of $Ni(CO)_2(Me_2P(CH_2)_nPMe_2)$ and $Ni(CO)_2(Ph_2P(CH_2)_nPPh_2)$ differ by 4×0.3 $cm^{-1} = 1.2$ cm^{-1}, whereas those of $Ni(CO)_3(PMe_3)$ and $Ni(CO)_2(PPh_3)$ differ by 3×1.7 $cm^{-1} = 5.1$ cm^{-1}). It is possible that bidentate and unidentate phosphines with phenyl groups are different electronically because they adopt different rotameric conformations of the phenyl groups relative to the metal–phosphorus bonding orbitals of π character.

Bite Angle Effects. One last point is that the length of the CH_2 backbone has a notable effect on the CO frequency. Thus, for example, adding one methylene unit to the backbone decreases ν(CO) by about as much (4 cm^{-1}) as changing all four substituents from Me to Et. Thus, bidentate phosphines appear to become slightly more electron donating as the $(CH_2)_n$ backbone becomes longer and the P–Ni–P angle becomes larger.

The origin of this effect can be probed by comparing the C–O vibrational frequencies and P–Ni–P angles of the complexes $Ni(CO)_2$(dmpe) and $Ni(CO)_2(PMe_3)_2$. These two compounds should be electronically similar, because the numbers of carbon atoms bound to each phosphorus atom are the same. The CO frequencies of these two complexes are 1996 and 1988 cm^{-1}, whereas the P–Ni–P angles are 90.1 and 110.7°, respectively. Thus, the unidentate phosphine complex follows the same trend as seen for the bidentate phosphines: for identical substituents, the CO stretching frequency decreases as the P–Ni–P angle increases. In other words, the "backbone length" effect is actually a "bite angle" effect.[45−47]

The bite angle can affect the orbital energy of the in-plane P–Ni–P d_{xy} metal–ligand hybrid orbital and, in turn, the donation of the metal fragment to the ancillary ligands. The exact amount by which the bite angle affects the bonding may be dependent on the geometry of the complex (e.g., tetrahedral vs octahedral).[48]

4. $NiH_2(R_2P(CH_2)_NPR_2)$ COMPLEXES

Geometries. No nickel(II) dihydrides of stoichiometry $NiH_2(PR_3)_2$ or $NiH_2(R_2P(CH_2)_nPR_2)$ have ever been reported, unlike the case for platinum(II), for which several *cis*-dihydride complexes are known.[49,50] Our DFT results show that, irrespective of the choice of the bidentate phosphine, the lowest energy structure of $NiH_2(R_2P(CH_2)_nPR_2)$ is a non-classical dihydrogen complex (Figure 3).[51] Data for these complexes are collected in Table 3.

The Ni–P distances in the dihydrogen complexes are typically 0.08 Å shorter than in the corresponding carbonyl complexes, possibly because the Ni center is formally three-coordinate instead of four-coordinate. This shortening causes the P–Ni–P angles for the hydride complexes to be 3–5° larger than for the carbonyl complexes. As seen in the carbonyl complexes, for molecules with identical substituents R, the Ni–P distance is 0.03 Å longer when the backbone has one CH_2 group vs when there are two or three (the latter have essentially identical Ni–P bond lengths).

The H–H distance and Ni–H distances are essentially insensitive to the number of CH_2 groups in the phosphine backbone but are sensitive to the substituents on phosphorus (Table 4). Specifically, the H–H distance is longer for alkyl substituents (e.g., ~0.948 Å for R = t-Bu) and shorter for fluorinated substituents (e.g., ~0.867 Å for R = CF_3). As seen for the carbonyl complexes, $Me_2P(CH_2)_nPMe_2$ and $Ph_2P(CH_2)_nPPh_2$ behave very similarly: the H–H bond distances in their nickel dihydrogen complexes are essentially equal.

The dependence of the H–H distance on the phosphine substituents is primarily an electronic effect, as shown by a plot of the H–H distance vs the CO stretching frequency in the corresponding nickel carbonyl complex bearing the same phosphine ligand (Figure 4). The H–H distance increases as the phosphine becomes a better electron donor.

dx.doi.org/10.1021/om200456j | *Organometallics* 2012, 31, 4122–4132

Table 3. Geometric Data for $Ni(H_2)(R_2P(CH_2)_nPR_2)$ Complexes Optimized with RI-BP86/def2-TZVP

label	n	R	H−H (Å)	P−Ni−P (deg)	$Ni-H_{av}$ (Å)	$Ni-P_{av}$ (Å)
pme3H2		Me	0.921	124.16	1.575	2.146
pph3H2		Ph	0.892	125.60	1.591	2.156
dtbupmH2	1	t-Bu	0.935	80.90	1.573	2.193
dtbupeH2	2	t-Bu	0.945	96.10	1.566	2.161
dtbuppH2	3	t-Bu	0.937	109.14	1.772	2.160
diprpmH2	1	i-Pr	0.946	79.00	1.567	2.176
diprpeH2	2	i-Pr	0.948	94.09	1.564	2.149
diprppH2	3	i-Pr	0.932	106.12	1.573	2.144
depmH2	1	Et	0.932	78.69	1.574	2.171
depeH2	2	Et	0.946	93.88	1.564	2.142
deppH2	3	Et	0.927	105.48	1.576	2.138
dmpmH2	1	Me	0.932	79.08	1.573	2.168
dmpeH2	2	Me	0.936	93.72	1.569	2.138
dmppH2	3	Me	0.930	105.68	1.573	2.134
dppmH2	1	Ph	0.926	78.39	1.577	2.169
dppeH2	2	Ph	0.921	93.22	1.577	2.143
dpppH2	3	Ph	0.919	106.76	1.579	2.141
dhpmH2	1	H	0.898	77.60	1.588	2.164
dhpeH2	2	H	0.901	92.72	1.588	2.125
dhppH2	3	H	0.898	103.36	1.589	2.120
domepmH2	1	OMe	0.898	78.21	1.594	2.128
domepeH2	2	OMe	0.898	93.47	1.595	2.105
domeppH2	3	OMe	0.891	106.20	1.597	2.102
dcf3ppH2	3	CF_3	0.866	104.55	1.619	2.098
dcf3pmH2	1	CF_3	0.866	79.38	1.617	2.130
dcf3peH2	2	CF_3	0.867	92.93	1.620	2.105
dfpmH2	1	F	0.870	77.76	1.616	2.114
dfpeH2	2	F	0.872	92.14	1.621	2.089
dfppH2	3	F	0.870	102.31	1.615	2.084

It is well established that transition-metal dihydrides can sometimes exist simultaneously in both classical dihydride and nonclassical dihydrogen forms,[52] and so we investigated whether the classical dihydride form of $NiH_2(R_2P(CH_2)_nPR_2)$ is a stable structure. We find that for some R groups (Me, Et, i-Pr, and t-Bu) a classical dihydride structure can be located on the potential energy surface as a local minimum. The lowest energy seen for this structure lies 0.4 kcal mol^{-1} above that of the corresponding nonclassical dihydrogen structure (Table 5). Therefore, for the phosphines tested in the present study (which cover a very large fraction of the possible electronic and steric parameter space), the dihydride form of $NiH_2(R_2P(CH_2)_nPR_2)$ is never the global minimum.

In the dihydride state, the H−H distances of 1.6−1.8 Å are about 0.9 Å longer than in the dihydrogen form. The average Ni−H distance decreases from 1.59 Å for the dihydrogen complex to 1.47 Å for the dihydride complexes. Accordingly, the H−Ni−H angle increases from ∼37° in the hydrogen complexes to ∼72° in the dihydride complexes. Other geometric changes are small: for example, the P−Ni−P angle increases by 3° relative to the dihydrogen complexes and the Ni−P distance increases by 0.01 Å.

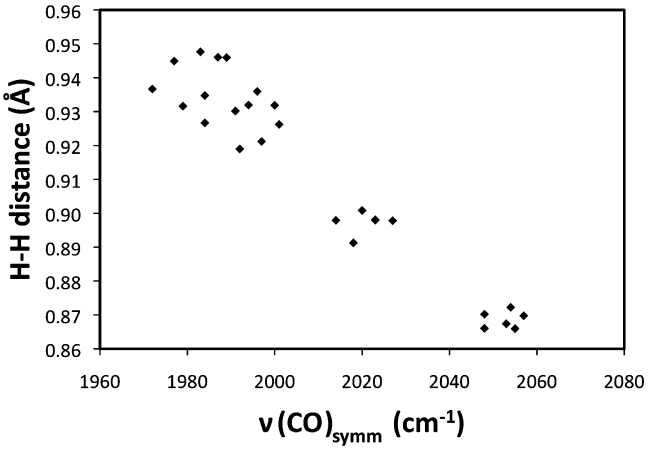

Figure 4. Plot of H−H distance (Å) in the dihydrogen complexes $Ni(H_2)(R_2P(CH_2)_nPR_2)$ versus calculated symmetric ν(CO) stretching frequencies of the corresponding $Ni(CO)_2(R_2P(CH_2)_nPR_2)$ complexes.

Interestingly, dihydride structures can be located on the potential energy surface only when the phosphine substituent is one of the alkyl groups mentioned above (i.e., Me, Et, i-Pr, or t-Bu), and not when it is one of the other substituents tested (Ph, H, OMe, CF_3, F). In order to explore this behavior in more detail, we calculated the energy of the three $Ni(H_2)(H_2P(CH_2)_nPH_2)$ complexes (n = 1−3) for a series of fixed H−H distances, allowing the rest of the structure to relax. The resulting plots of the potential energy surface along this reaction coordinate (Figure 5) show the presence of only one local minimum, which corresponds to the dihydrogen structure (H−H = 0.9 Å). For the complexes of these phosphines, which bear hydrogen substituents on phosphorus, there is no local minimum but rather an "incipient minimum" (a lessening of the gradient) near H−H distances of 1.5−1.8 Å. These latter distances are characteristic of classical dihydride complexes.

If we compute the corresponding plot of the potential energy vs H−H distance for a nickel complex bearing one of the alkyl substituents, $NiH_2(Me_2PCH_2PMe_2)$, we find (Figure 5) that there is a very flat local minimum in the potential energy surface near the dihydride distance (1.7 Å). The general trend here is as expected: phosphines bearing electron-donating substituents such as alkyl groups increase the stability of a classical dihydride structure relative to a nonclassical dihydrogen alternative.[53] In the next section, we explore the reasons for this correlation.

5. BONDING ANALYSIS

In order to probe the nickel−hydrogen bonding in the $NiH_2(R_2P(CH_2)_nPR_2)$ complexes, we have analyzed the electron density distributions within both the nonclassical

Table 4. H−H Bond Distances (Å) for $NiH_2(R_2P(CH_2)_nPR_2)$ Complexes as a Function of the Substituent R

	R								
	t-Bu	i-Pr	Et	Me	Ph	H	OMe	CF_3	F
n = 1	0.935	0.946	0.932	0.932	0.926	0.898	0.898	0.866	0.870
n = 2	0.945	0.948	0.946	0.936	0.921	0.901	0.898	0.867	0.872
n = 3	0.937	0.932	0.927	0.930	0.918	0.898	0.891	0.866	0.870

dx.doi.org/10.1021/om200456j | Organometallics 2012, 31, 4122−4132

Table 5. H−H Bond Distances (Å) and Vibration-Corrected Energy, ΔE (kcal mol^{-1}), of the Dihydride Structure of $NiH_2(R_2P(CH_2)_nPR_2)$ Relative to the Energy of the Dihydrogen Structure

	R = t-Bu		R = i-Pr		R = Et		R = Me	
	H−H (Å)	ΔE (kcal mol^{-1})	H−H (Å)	ΔE (kcal mol^{-1})	H−H (Å)	ΔE (kcal mol^{-1})	H−H (Å)	ΔE (kcal mol^{-1})
n = 1	1.630	1.4	1.734	0.7	1.640	1.5	1.599	1.4
n = 2	1.746	1.1	1.774	0.7	1.801	0.4	1.762	1.0
n = 3	1.625	1.1	1.648	1.4	1.643	1.6	1.752	1.2

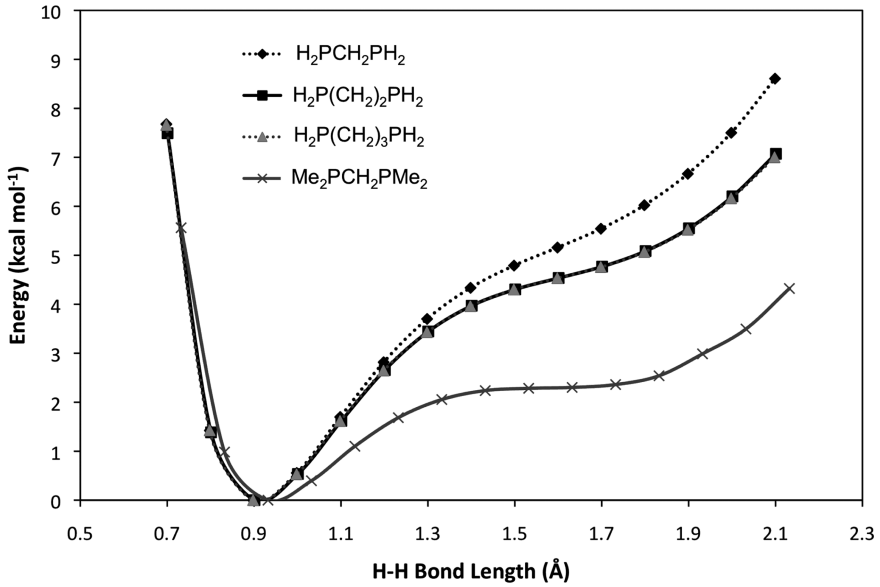

Figure 5. Relaxed scan of the energy of $Ni(H_2)(R_2P(CH_2)_nPR_2)$ complexes as a function of the H−H distance using BP86/def2-TZVP. The structure was reoptimized at each scan point, and the energies are reported relative to that of the global minimum.

dihydrogen and classical dihydride forms of these molecules. Three methods have been employed: Bader's atoms in molecule (AIM) approach, natural bond orbital analysis (NBO), and energy decomposition analysis (EDA).

Contour line diagrams of the Laplacian of the electron density for the dihydrogen and dihydride forms of $NiH_2(Me_2PCH_2PMe_2)$ show that, as expected, the Ni−H interactions are different.[54] In the dihydrogen complex (Figure 6a), there is one bond path between the nickel atom and the H−H unit, but in the dihydride tautomer there are two such bond paths, one to each hydrogen atom (Figure 6b). For the Ni−dihydrogen complex, a bond path also connects the two hydrogen atoms; this bond path is slightly curved in the direction toward the nickel center. At the critical points in the Ni−H bonds of the dihydride form, the calculated Laplacian of the electron density ($\nabla^2\rho$ = 0.198 au) is somewhat larger than values calculated for the nonlinear triatomic dihydride NiH_2 ($\nabla^2\rho$ = 0.057−0.177 au) for a variety of functionals and correlated methods.[55] This finding suggests that the electron density is somewhat more depleted in the Ni−H bonds of the present phosphine complexes, as might be expected owing to the larger number of ligands.[56]

NBO analysis confirms that species with H−H distances less than 1.0 Å possess three-center bonds between Ni and the H_2 ligand, whereas complexes with H−H distances greater than 1.0 Å possess two Ni−H bonds, one to each hydrogen atom.

The nickel-based frontier orbitals on the L_2Ni fragment that interact with the hydrogen atoms should be a filled d orbital (or hybrid) of π symmetry and an empty p orbital (or hybrid) of σ symmetry (Figure 7). The relative energies of these two

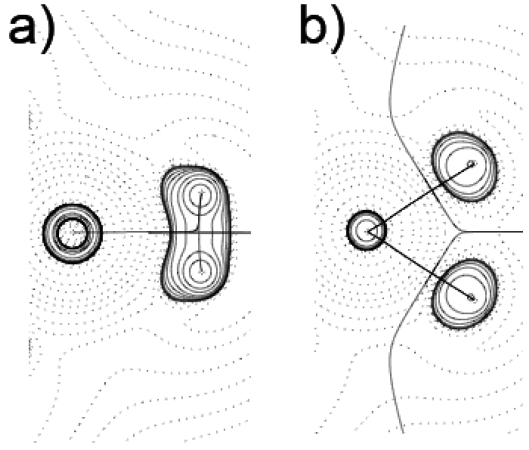

Figure 6. Contour plots of the Laplacian of the electron density, $\nabla^2\rho$, in the mean molecular plane, for (a) the dihydrogen and (b) the dihydride forms of $NiH_2(Me_2PCH_2PMe_2)$. The nickel atom is on the left in both plots; the phosphine atoms are not shown. Solid lines indicate areas of charge concentration ($\nabla^2\rho < 0$), whereas dashed lines show areas of charge depletion ($\nabla^2\rho > 0$). The nickel in (a) has a slightly different structure appearance because the Ni−H_2 bond (a) lies out of the Ni−P plane whereas the Ni−H bonds (b) lie in the Ni−P plane. In (a), the apparent sharp turn of the bond path toward the upper hydrogen atom is a numerical artifact. For a similar result, see Figure 3.1f on page 57 of Bader's book.[12]

frontier orbitals in the L_2Ni fragment are $E(\pi) < E(\sigma)$. As the phosphine becomes more electron rich, the energies of both of these frontier orbitals on the L_2Ni fragment should increase due to shielding of the nuclear charge of the nickel atom. Increasing

dx.doi.org/10.1021/om200456j | Organometallics 2012, 31, 4122−4132

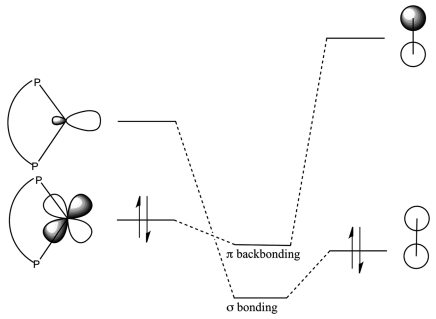

Figure 7. Diagram of σ and π interactions between the Ni-($R_2PCH_2PR_2$) fragment and H_2 molecule.

the energy of both Ni frontier orbitals will have two effects: the σ donation from H_2 to Ni will decrease, whereas the π back-bonding contribution from Ni to H_2 will increase. In the limit of a very electron donating phosphine, the π contribution should be very strong, and the dihydride form of the complex will be stabilized relative to the molecular dihydrogen form.

The derived Kohn–Sham orbitals shown in Figure 8 support this view. Taking the z axis along the Ni–H_2 bond and the xz plane as that defined by the nickel and two hydrogen atoms, the two highest occupied molecular orbitals (HOMO 13A′ and HOMO-1 7A″) are primarily metal-based d_{xy} and $d_{x^2-y^2}$ orbitals. The 6A″ orbital is the Ni–H_2 π back-bonding interaction, and it involves mixed d_{xz}/p_x character on Ni. The Ni–H_2 σ interactions are distributed over three lower energy orbitals, 8A′, 7A′, and 6A′ (Table 5 in the Supporting Information); apart from core orbital contributions from the phosphine ligands, each involves mostly hydrogen s character with small amounts of Ni d_{z^2}/p_z character.

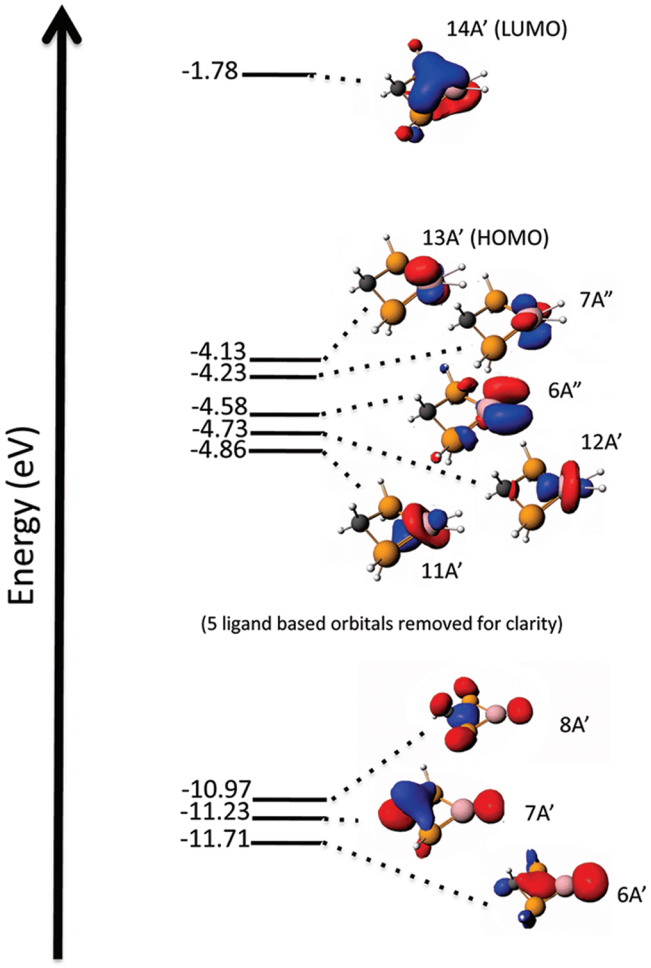

Figure 8. Selected Kohn–Sham orbitals for $NiH_2(H_2PCH_2PH_2)$ visualized at 0.05 e Å^{-3}. The nickel atom is pink, phosphorus atoms are orange, and carbon atoms are black; hydrogen atoms are depicted as smaller white spheres. The Ni–H_2 π back-bonding orbital is orbital 6A″, and the Ni–H_2 σ orbitals are orbitals 6A′, 7A′, and 8A′. The remaining orbitals are shown in the Supporting Information.

To explore the relative importance of σ and π metal–H_2 bonding, we used structures optimized with the Amsterdam Density Functional (ADF) to carry out energy decomposition analyses (EDA) on selected dihydrogen complexes (Table 6). In both the C_2 and C_s point groups, the frontier orbitals of the (PP)Ni and H_2 fragments involved in forming the Ni–H_2 bond(s) transform differently: one is symmetric with respect to the 2-fold rotation or mirror plane and the other is antisymmetric. As a result of the σ and π contributions to the Ni–H_2 bonding, their relative contributions to the overlap energies can be differentiated.

The EDA results show that the relative σ vs π contribution depends on the nature of the substituents on the bidentate phosphine. For phosphines with R = t-Bu, i-Pr, Et, Me, Ph, H, OMe (i.e., the more electron donating substituents), metal to H_2 π back-donation is the dominant orbital component. In contrast, for R = F, CF_3 (i.e., the more electron withdrawing substituents), H_2 to metal σ donation is dominant. There is also a strong correlation between the relative σ and π contributions and the H–H distance (Figure 9). The EDA results clearly indicate that long H–H distances are seen when the M → (H_2) π back-donation dominates over H_2 → M σ donation. This conclusion agrees with the results of previous theoretical investigations of metal–dihydrogen interactions.[17,58]

Because the H–H distance correlates both with the σ vs π makeup of the M–H_2 bonding and with the electronic nature of the phosphine, it should be expected that the last two parameters are correlated with one another. Indeed, this is so (Figure 10): the percent π contribution in the Ni–H_2 bond increases as the carbonyl stretching frequency in the analogous $Ni(CO)_2(R_2PCH_2PR_2)$ complex decreases (i.e., as the phosphine becomes more electron rich). These correlations are completely consistent with the orbital picture in Figure 7. Similar correlations between the percentage π contribution in a metal–carbonyl bond and the CO stretching frequency have previously been described.[7,57]

As the number of carbon atoms in the backbone of the phosphine is increased from one to three (Table 7), the H–H distance remains approximately constant as does the percent orbital and percent electrostatic contributions. Interestingly, the percent σ donation is 45% for nickel dihydrogen complexes bearing phosphines with two-carbon backbones (dhpe) vs 48% for analogous complexes with one- or three-carbon backbones (dhpm and dhpp).

A recent paper reported that the lability of a H_2 ligand in a ruthenium complex is sensitive to the electronic character of the bidentate phosphine.[6] Electron-withdrawing substituents rendered the H_2 complex susceptible to substitution by H_2O, whereas electron-donating substituents stabilized the H_2 complex. The authors suggested that electron-donating substituents on the phosphine increased the π back-donation into the M–H_2 bond, increasing the M–H_2 bond dissociation energy. Our EDA results (Table 6) are consistent with this

dx.doi.org/10.1021/om200456j | Organometallics 2012, 31, 4122–4132

Table 6. EDA Data for $NiH_2(R_2PCH_2PR_2)$ Dihydrogen Complexes at BP86/TZ2P (ZORA): Distances in Å and Energies in kcal mol^{-1}

	R								
	t-Bu[a]	i-Pr	Et	Me	Ph	H	OMe	CF_3	F
molecular symmetry	C_s	C_s	C_s	C_s	C_s	C_s	C_s	C_s	C_s
H−H	0.980	0.996	0.959	0.958	0.962	0.915	0.916	0.877	0.879
ΔE_{int}	−41.27	−44.67	−39.74	−39.64	−39.83	−34.05	−33.8	−28.19	−28.07
ΔE_{Pauli}	100.35	97.87	92.13	92.4	92.59	83.2	81.88	74.95	74.86
ΔE_{elstat}[b]	−82.54 (58.3)	−83.18 (58.4)	−76.93 (58.3)	−77.18 (58.5)	−77.61 (58.6)	−68.91 (58.8)	−67.83 (58.6)	−60.34 (58.5)	−59.88 (58.2)
ΔE_{orb}[b]	−59.09 (41.7)	−59.36 (41.6)	−54.94 (41.7)	−54.86 (41.5)	−54.8 (41.4)	−48.34 (41.2)	−47.85 (41.4)	−42.8 (41.5)	−43.04 (41.8)
ΔE_{σ}[c]	−25.32 (42.8)	−24.07 (40.5)	−23.92 (43.5)	−24.00 (43.8)	−23.64 (43.1)	−23.26 (48.1)	−22.73 (47.5)	−23.72 (55.4)	−23.68 (55.0)
ΔE_{π}[c]	−33.77 (57.2)	−35.29 (59.6)	−31.03 (56.5)	−30.86 (56.2)	−31.16 (56.9)	−25.09 (51.9)	−25.11 (52.5)	−19.07 (44.6)	−19.36 (45.0)
ΔE_{prep}	19.01	19.94	15.96	16.15	15.69	11.40	11.63	8.03	8.67
$\Delta E = -D_e$	−22.26	−24.73	−23.78	−23.49	−24.14	−22.65	−22.17	−20.16	−19.40

[a] dtBupm in C_s symmetry exhibits one large imaginary frequency of −43 cm^{-1}. [b] Values in parentheses are percentage contributions to the total attractive interactions $\Delta E_{elstat} + \Delta E_{orb}$. [c] Values in parentheses are percentage σ and π contributions to the total orbital interactions ΔE_{orb}.

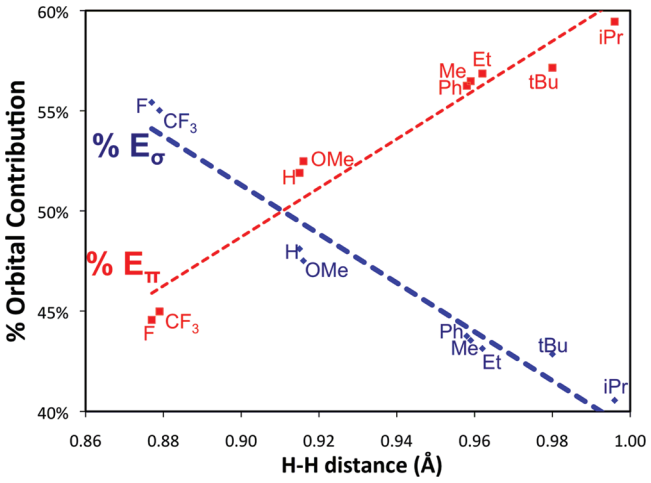

Figure 9. Plot of the percent σ orbital contribution (blue diamonds) and percent π orbital contribution (red squares) to the Ni−H_2 bond versus the H−H distance (Å).

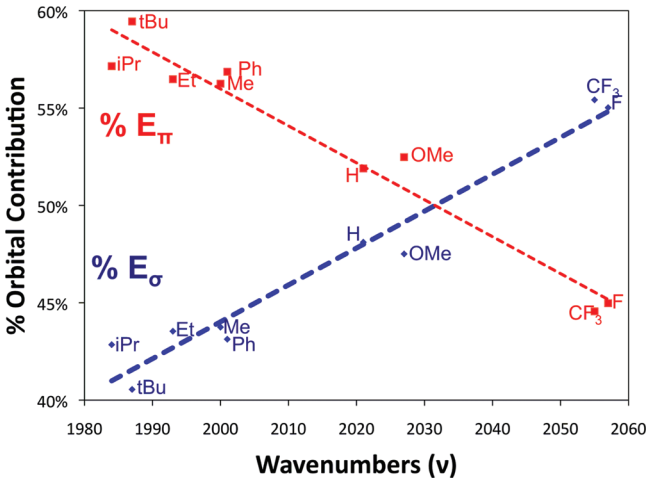

Figure 10. Plot of the percent σ orbital contribution (blue diamonds) and percent π orbital contribution (red squares) to the Ni−H_2 bond in $Ni(H_2)(R_2P(CH_2)_nPR_2)$ versus the calculated symmetric CO stretching frequency (cm^{-1}) of the corresponding $Ni(CO)_2(R_2P(CH_2)_nPR_2)$ complex. EDA values are from ADF calculations, whereas CO stretching frequencies are from Turbomole calculations.

trend: nickel dihydrogen complexes bearing electron-withdrawing phosphines, such as those with F and CF_3 substituents, have lower H_2 dissociation energies (~19 kcal mol^{-1}) than do complexes bearing electron-donating phosphines, such as t-Bu and i-Pr (~23 kcal mol^{-1}).

CONCLUSIONS

The carbonyl stretching frequencies of $Ni(CO)_2(R_2P(CH_2)_nPR_2)$ complexes depend both on the substituents (R) on phosphorus and on the length of the $(CH_2)_n$ backbone. The substituent trends seen are generally similar to those determined for unidentate phosphines, although there is evidence that bidentate and unidentate phosphines with phenyl groups are different electronically, possibly owing to the different rotameric conformations of the phenyl groups relative to the metal−phosphorus bonding orbitals of π character. The effect of the length of the CH_2 backbone can be traced simply to changes in the P−Ni−P angle, which changes the overlap with the d orbitals on the metal center.

An investigation of the structures of a series of nickel hydride complexes of stoichiometry $NiH_2(R_2P(CH_2)_nPR_2)$ shows that, irrespective of the phosphine, all of these complexes adopt ground-state structures containing a nonclassical dihydrogen ligand. For bidentate phosphines that are strongly donating, however, a classical *cis*-dihydride structure is only slightly higher in energy than the global minimum. For phosphines that are less electron donating, this structure is no longer a local minimum but instead is an inflection point on the potential energy surface. In this system, methyl and phenyl substituents again appear to be more similar to one another electronically than they are for unidentate phosphines.

We propose that the trends seen in the systems studied above are likely to be general and should be useful in understanding differences sometimes seen[6,58−60] in the reactivities of transition-metal complexes bearing bidentate complexes.

dx.doi.org/10.1021/om200456j | *Organometallics* 2012, 31, 4122−4132

Table 7. EDA Data for $NiH_2(H_2P(CH_2)_nPH_2)$ Complexes, Where n = 1−3: at BP86/TZ2P (ZORA): Distances in Å and Energies in kcal mol^{-1}

	phosphine		
	$H_2PCH_2PH_2$	$H_2P(CH_2)_2PH_2$	$H_2P(CH_2)_3PH_2$
molecular symmetry	C_s	C_2	C_s
H−H	0.915	0.917	0.916
ΔE_{int}	−34.05	−35.24	−33.88
ΔE_{Pauli}	83.2	80.6	85.26
ΔE_{elstat} [a]	−68.91 (58.8)	−68.70 (59.3)	−70.72 (59.4)
ΔE_{orb} [a]	−48.34 (41.2)	−47.14 (40.7)	−48.41 (40.6)
ΔE_{σ} [b]	−23.26 (48.1)	−21.05 (44.6)	−23.69 (48.9)
ΔE_{π} [b]	−25.09 (51.9)	−26.09 (55.4)	−24.72 (51.1)
ΔE_{prep}	11.40	11.76	13.02
$\Delta E = -D_e$	−22.65	−23.48	−20.86

[a]Values in parentheses are percentage contributions to the total attractive interactions $\Delta E_{elstat} + \Delta E_{orb}$. [b]Values in parentheses are percentage σ and π contributions to the total orbital interactions ΔE_{orb}.

■ ASSOCIATED CONTENT

Supporting Information

Tables and figures giving further details of the calculations. This material is available free of charge via the Internet at http://pubs.acs.org.

■ AUTHOR INFORMATION

Corresponding Author

*E-mail: girolami@scs.illinois.edu (G.S.G.); frenking@chemie.uni-marburg.de (G.F.).

■ ACKNOWLEDGMENTS

This research was supported in part by the National Science Foundation through Grant CHE07-50422 to G.S.G. Calculations were performed with TeraGrid resources provided by the National Center for Supercomputing Applications and with Hochschulrechenzentrum resources of the Philipps-Universität Marburg. C.F.L. gratefully acknowledges the support of the German-American Fulbright Commission for funding her time with the group of G.F.

■ REFERENCES

(1) Tolman, C. A. *Chem. Rev.* **1988**, *77*, 313−348.
(2) Gusev, D. G. *J. Am. Chem. Soc.* **2004**, *126*, 14249−14257.
(3) Hay, P. J. *J. Am. Chem. Soc.* **2002**, *109*, 705−710.
(4) Perrin, L.; Clot, E.; Eisenstein, O.; Loch, J.; Crabtree, R. H. *Inorg. Chem.* **2001**, *40*, 5806−5811.
(5) Massera, C.; Frenking, G. *Organometallics* **2003**, *22*, 2758−2765.
(6) Szymczak, N. K.; Braden, D. A.; Crossland, J. L.; Turov, Y.; Zakharov, L. N.; Tyler, D. R. *Inorg. Chem.* **2009**, *48*, 2976−2984.
(7) Frenking, G.; Loschen, C.; Krapp, A.; Fau, S.; Strauss, S. H. *J. Comput. Chem.* **2007**, *28*, 117−126.
(8) Gusev, D. G. *Organometallics* **2009**, *28*, 763−770.
(9) Reed, A. E.; Weinstock, R. B.; Weinhold, F. *J. Chem. Phys.* **1985**, *83*, 735−746.
(10) Weinhold, F.; Landis, C. R. *Valency and Bonding: A Natural Bond Orbital Donor-Acceptor Perspective*; Cambridge University Press: New York, 2005.
(11) Reed, A. E.; Curtiss, L. A.; Weinhold, F. *Chem. Rev.* **2002**, *88*, 899−926.
(12) Bader, R. F. W. *Atoms in Molecules: A Quantum Theory*; Clarendon Press: Oxford, U.K., 1990.
(13) Tognetti, V.; Joubert, L.; Cortona, P.; Adamo, C. *J. Phys. Chem. A* **2009**, *113*, 12322−12327.
(14) Frenking, G.; Fröhlich, N. *Chem. Rev.* **2000**, *100*, 717−774.
(15) Antonova, N. S.; Carbó, J. J.; Poblet, J. M. *Organometallics* **2009**, *28*, 4283−4287.
(16) Frenking, G.; Wichmann, K.; Froehlich, N.; Loschen, C.; Lein, M.; Frunzke, J.; Rayon, V. M. *Coord. Chem. Rev.* **2003**, *238*−*239*, 55−82.
(17) Lein, M.; Frenking, G. In *Theory and Applications of Computational Chemistry: The First 30 Years*, 1st ed.; Frenking, G., et al., Eds.; Elsevier Science: New York, 2005, pp 291−372.
(18) Esterhuysen, C.; Frenking, G. *Theor. Chem. Acc.* **2004**, *111*, 381−389.
(19) Kovacs, A.; Esterhuysen, C.; Frenking, G. *Chem. Eur. J.* **2005**, *11*, 1813−1825.
(20) Bickelhaupt, F. M.; Baerends, E. J. In *Reviews in Computational Chemistry*, 1st ed.; Wiley-VCH: New York, 2000; Vol. *15*, pp 1−86.
(21) te Velde, G.; Bickelhaupt, F. M.; Baerends, E. J.; Guerra, C. F.; van Gisbergen, S. J. A.; Snijders, J. G.; Ziegler, T. *J. Comput. Chem.* **2001**, *22*, 931−967.
(22) Morokuma, K. *J. Chem. Phys.* **1971**, *55*, 1236−1244.
(23) Fernandez, I.; Frenking, G. *J. Org. Chem.* **2006**, *71*, 2251−2256.
(24) Ahlrichs, R.; Bär, M.; Häser, M.; Horn, H.; Kölmel, C. *Chem. Phys. Lett.* **1989**, *162*, 165−169.
(25) Perdew, J. P. *Phys. Rev. B* **1986**, *33*, 8822−8824.
(26) Becke, A. D. *Phys. Rev. A* **1988**, *38*, 3098−3100.
(27) Weigend, F. *Phys. Chem. Chem. Phys.* **2002**, *4*, 4285−4291.
(28) Weigend, F.; Ahlrichs, R. *Phys. Chem. Chem. Phys.* **2005**, *7*, 3297−3305.
(29) Recent work: (a) Parameswaran, P; Frenking, G. *Chem. Eur. J.* **2009**, *15*, 8807−8816. (b) Parameswaran, P; Frenking, G. *Chem. Eur. J.* **2009**, *15*, 8817−8824. (c) Erhardt, S.; Frenking, G. *J. Organomet. Chem.* **2009**, *694*, 1091−1100. (d) Cadenbach, T; Bollermann, T.; Gemel, C.; Fernández, I.; von Hopffgarten, M.; Frenking, G.; Fischer, R. *Angew. Chem., Int. Ed.* **2008**, *47*, 9150−9154. (e) Mörschel, P.; Janikowski, J.; Hilt, G.; Frenking, G. *J. Am. Chem. Soc.* **2008**, *130*, 8952−8966. (f) Cadenbach, T.; Gemel, C.; Bollermann, T.; Fernández, I.; Frenking, G.; Fischer, R. A. *Chem. Eur. J.* **2008**, *14*, 10789−10796. (g) Fernández, I.; Frenking, G. *Chem. Eur. J.* **2007**, *13*, 5873−5884. (h) Krapp, A.; Frenking, G. *J. Am. Chem. Soc.* **2008**, *130*, 16646−16658. (i) Krapp, A.; Pandey, K. K.; Frenking, G. *J. Am. Chem. Soc.* **2007**, *129*, 7596−7610. (j) Nechaev, M. S.; Rayón, V. M.; Frenking, G. *J. Phys. Chem. A* **2004**, *108*, 3134−3142. (k) Frunzke, J.; Loschen, C.; Frenking, G. *J. Am. Chem. Soc.* **2004**, *126*, 3642−3652. For further validations of the BP86 method for analysis of dihydride/dihydrogen complexes, see sections VI and VII of the Supporting Information.
(30) Jacobsen, H. *J. Phys. Chem. A* **2002**, *106*, 6189−6192.
(31) Reviews: (a) Boehme, C.; Uddin, J.; Frenking, G. *Coord. Chem. Rev.* **2000**, *197*, 249. (b) Diedenhofen, M.; Wagener, T.; Frenking, G. In *Computational Organometallic Chemistry*; Cundari, T., Ed.; Marcel Dekker: New York, 2001; p 69. (c) Fröhlich, N.; Frenking, G. In *Theoretical Thermochemistry*; Cioslowsky, J., Ed.; Kluwer Academic: New York, 2001; p 199. (d) Maseras, F.; Lledós, A.; Clot, E.; Eisenstein, O. *Chem. Rev.* **2000**, *100*, 601−636.
(32) Frisch, M. J.; et al. *Gaussian03, Rev. E.01*; Gaussian, Inc., Wallingford, CT, 2004.
(33) In *ADF2007.01*; SCM, Theoretical Chemistry, Vrijie Universiteit Amsterdam, Amsterdam, 2007.
(34) van Lenthe, E.; Baerends, E. J.; Snijders, J. G. *J. Chem. Phys.* **1993**, *99*, 4597−4610.
(35) van Lenthe, E.; Baerends, E. J.; Snijders, J. G. *J. Chem. Phys.* **1994**, *101*, 9783−9792.
(36) van Lenthe, E.; Ehlers, A.; Baerends, E.-J. *J. Chem. Phys.* **1999**, *110*, 8943−8953.
(37) Our own EDA program is unable to differentiate between σ and π bonding. Therefore ,we had to use ADF, which has Slater basis functions. Previous work by us has shown that the differences between the results which are obtained using Slater and Gaussian functions are

negligible if the same basis set quality is used. ZORA is automatically included in the ADF calculations, although relativistic effects are negligible for elements of the first transition-metal row.
(38) van Hecke, G. R.; Horrocks, W. D. *Inorg. Chem.* **1966**, *5*, 1968−1974.
(39) Trebbe, R.; Goddard, R.; Rufinska, A.; Seevogel, K.; Pörschke, K. R. *Organometallics* **1999**, *18*, 2466−2472.
(40) Ficker, R.; Hiller, W. Regius, T. C.; Hofmann, R. *Z. Kristallogr.* **1996**, *211*, 62−63.
(41) Jonas, V.; Frenking, G.; Reetz, M. T. *J. Am. Chem. Soc.* **2002**, *116*, 8741−8753.
(42) Booth, G.; Chatt, J. *J. Chem. Soc.* **1965**, 3238−3241.
(43) van Hecke, G. R.; Horrocks, W. D. *Inorg. Chem.* **1966**, *5*, 1960−1968.
(44) Chatt, J.; Hart, F. A. *J. Chem. Soc.* **1960**, 1378−1389.
(45) Birkholz, M. N.; Freixa, Z.; van Leeuwen, P. W. N. M. *Chem. Soc. Rev.* **2009**, *38*, 1099−1118.
(46) van Zeist, W. J.; Visser, R.; Bickelhaupt, F. *Chem. Eur. J.* **2009**, *15*, 6112−6115.
(47) Freixa, Z.; van Leeuwen, P. W. N. M. *Dalton Trans.* **2003**, 1890−1901.
(48) We thank a reviewer for pointing this out.
(49) Yoshida, T.; Yamagata, T.; Tulip, T. H.; Ibers, J. A.; Otsuka, S. *J. Am. Chem. Soc.* **1978**, *100*, 2063−2073.
(50) Moulton, C. J.; Shaw, B. L. *J. Chem. Soc., Chem. Commun.* **1976**, 365−366.
(51) Lin, Z.; Hall, M. B. *J. Am. Chem. Soc.* **2002**, *114*, 6574−6575.
(52) Said, R. B.; Tangour, B.; Barthelat, J. C. *J. Mol. Struct/(THEOCHEM)* **2008**, *857*, 115−122.
(53) Hall, M. B.; Lin, Z. *Coord. Chem. Rev.* **1994**, *135*−*136*, 845−879.
(54) Popelier, P. L. A. *J. Phys. Chem. A* **1998**, *102*, 1873−1878.
(55) Platts, J. A. *J. Mol. Struct. (THEOCHEM)* **2001**, *545*, 111−118.
(56) It is not necessarily true that the bond path always connects an attractor with another attractor; it is also possible that bond path can connect an attractor with a (3,−1) critical point; see: *J. Am. Chem. Soc.* **1986**, *108*, 5732−5731. Figure 1b in this paper shows a bond path that connects a metal atom with the midpoint of a C−-C bond. A theoretical analysis of such cases is discussed by Bader (ref 12, p 66, Figure 3.4). It is also not true that two atoms, whose atomic basins are in contact, need to have a bond path. This is clearly demonstrated in Figure 3.1b on p 56 of the book by Bader.
(57) Dapprich, S.; Frenking, G. *Angew. Chem., Int. Ed. Engl.* **1995**, *34*, 354−357.
(58) Kabir, S. E.; Mottalib, M. A.; Hossain, G. M. G.; Nordlander, E.; Rosenberg, E. *Polyhedron* **2006**, *25*, 95−104.
(59) Eglin, J. L.; Valente, E. J.; Winfield, K. R.; Zubkowski, J. D. *Inorg. Chim. Acta* **1996**, *245*, 81−85.
(60) Wassenaar, J.; Jansen, E.; van Zeist, W. J.; Bickelhaupt, F. M.; Siegler, M. A.; Spek, A. L.; Reek, J. N. H. *Nat. Chem.* **2010**, *2*, 417−421.